Original Contribution

Obere Extremität 2021 · 16:120–129
https://doi.org/10.1007/s11678-021-00622-3
Received: 2 October 2020
Accepted: 4 January 2021
Published online: 28 January 2021

Daniel P. Berthold[1,2] · Lukas N. Muench[1,2] · Ryan Bell[1] · Colin Uyeki[1] · Kane Zenon[2] · Augustus D. Mazzocca[2] · Elifho Obopilwe[2] · Mark P. Cote[2] · Andreas B. Imhoff[2] · K. Beitzel[2,3]

[1] Department of Orthopedic Surgery, University of Connecticut, Farmington, USA
[2] Department of Orthopedic Sports Medicine, Technical University of Munich, Munich, Germany
[3] Arthroscopy and Orthopedic Sportsmedicine, ATOS Orthoparc Clinic, Cologne, Germany

Biomechanical consequences of isolated, massive and irreparable posterosuperior rotator cuff tears on the glenohumeral joint

A dynamic biomechanical investigation of rotator cuff tears

Background

The glenohumeral joint has the greatest range of motion (ROM) of any joint in the human body; however, this is accompanied by an increased risk of joint instability [21]. As such, close and complex interactions between dynamic and static stabilizers of the shoulder girdle are critical for producing a biomechanically complex system ensuring the shoulder has a sufficient ROM in multiple planes.

Massive rotator cuff tears (RCT) represent almost 40% of all RCT and are often associated with persistent defects and worse clinical outcomes [3, 15]. These defects include persistent pain, loss of ROM, and insufficient function, which all may significantly affect the patients' quality of life [32].

A solid understanding of both native and defect shoulder kinematics is key to approaching rotator cuff surgery. Along with the aforementioned stabilizers ensuring muscular balance and rotational function, the anatomy of the rotator cuff applies a compressive load to the glenohumeral joint throughout ROM. Additionally, the muscular force couple provides glenohumeral joint stability and contributes to humeral head centration [31].

Patients with tears of the superior portion of the rotator cuff who present with stable fulcrum kinematics often demonstrate preserved essential force couples in the coronal and transverse planes [5]. However, when facing massive tears of the superior and posterior cuff, unstable fulcrum kinematics may occur, thus leading to uncoupling of the essential force couples [5]. Additionally, superior humeral head migration and altered intra-articular joint pressure can lead to severe humeral head and/or glenoid osteoarthritis, which may result in severe pain and insufficient joint function. However, to date there is limited detailed information on the biomechanical consequences of isolated and massive, non-retracted RCT and massive, retracted posterosuperior RCT in the glenohumeral joint.

The purpose of the study was to assess the biomechanical consequences of isolated, massive, non-retracted RCT (according to Patte I) and irreparable, retracted posterosuperior RCT (Patte III) on the glenohumeral joint using a validated, dynamic shoulder testing system. The authors hypothesized that: (1) in a dynamic biomechanical set-up, RCT lateral to the rotator cable can be sufficiently compensated by the remaining intact cuff, and (2) irreparable, retracted posterosuperior RCT medial to the rotator cable have significant effects on the glenohumeral joint leading to decreased overall shoulder function.

Materials and methods

This study was reviewed by the institutional review board (IRB) of the University of Connecticut, via the Human Research Determination Form, and it was concluded that no IRB approval was required. Eight male, fresh-frozen, independent cadaveric shoulder specimens were obtained from Medcure Inc. (Portland, OR, USA): three right, and five left shoulders. The mean age was 53.4 ± 14.2 years (range: 20–64 years). All specimens underwent visual and radiographic inspection to detect and exclude those with moderate-to-severe osteoarthritis (Kellgren–Lawrence Grade 2 or more), bony defects, tears of the rotator cuff tendons or capsule, or joint contractures. As such, no specimen had to be excluded.

Specimen preparation

Specimen preparation was performed according to a previously described method [1, 11, 12, 28]. Prior to dissection, specimens were thawed overnight at room

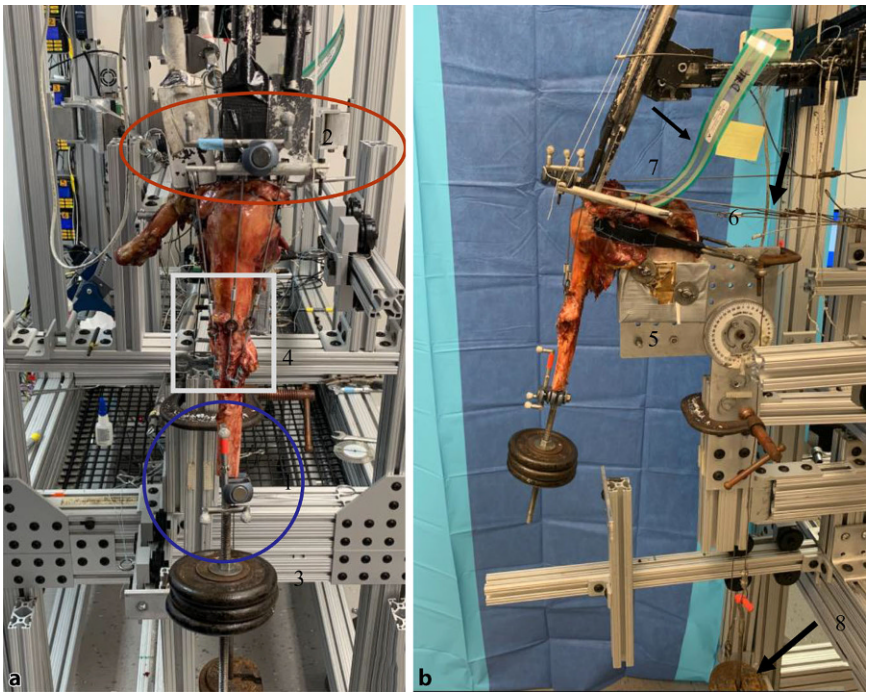

Fig. 1 ▲ Figure demonstrating the dynamic shoulder simulator **a** *1*. A moving triad is mounted to the humeral shaft with its longitudinal axis in line with the center of the humeral head *2*. Stationary triad placed on the acromion. *3*. A steel rod is cemented into the distal humerus and loaded with 1.7 kg, 30 cm distal from the center of the humeral head to simulate native forearm weight. *4*. Anchor loops sutured to the tendinous insertions of the anterior, middle, and posterior portions of the deltoid tendon at the deltoid tuberosity using a locking running stitch to allow for attachment of an individual shoulder simulator actuator to each of the three deltoid heads. **b** *5*. The specimen is mounted to the simulator on a jig with6 degrees of freedom with the scapula in 10° of anteflexion, 10° superior tilt of the glenoid, resulting in a 110° angle between the scapular spine and vertical axis. *6*. The cable attached to the supraspinatus tendon is positioned at 10° from the horizontal. *7*. The Tekscan sensor is placed underneath the acromion and the free end is connected to the measuring device. *8*. The subscapularis and infraspinatus/teres minor unit are loaded statically with a 1.36-kg hanging weight, allowing for a balanced abduction motion

temperature. Thawed specimens were then dissected free of skin as well as subcutaneous and muscle tissue, while preserving the rotator cuff muscles and the coracoacromial ligament. The anterior, middle, and posterior portions of the deltoid tendon were detached from the muscle belly at the deltoid tuberosity. Anchor loops were sutured to the tendinous insertions of the three portions of the deltoid using a locking running stitch (No. 2 FiberWire, Arthrex Inc., Naples, FL, USA), allowing for the attachment of each of the three deltoid heads to an individual shoulder simulator actuator [1, 12, 28]. Next, the rotator cuff muscles, including the supraspinatus (SSP), subscapularis (SSC), infraspinatus (ISP), and teres minor (TM), were sharply released from the scapula and separated from the underlying capsule. As previously described and validated, the ISP and TM were simulated as one unit [1, 12, 17, 28].

Next, the individual rotator cuff tendons were sutured to pulley-straps using No. 2 FiberWire to avoid pull-through during load application. The scapular body was fixed with bone cement poured in a custom rectangular box with the medial border aligned perpendicular to the ground and the glenoid tilted 10° superiorly [1, 12, 16, 28, 34]. Next, a steel rod was cemented into the distal humerus and loaded with 1.7 kg, 30 cm distal from the center of the humeral head, to simulate native forearm weight [17, 34]. As previously described, the glenohumeral joint capsule was vented by opening the rotator interval, in order to prevent changes during testing [1, 12, 28].

Testing set-up

A previously validated dynamic shoulder simulator was utilized to test the cadaveric shoulders for this study ([1, 10–12, 16, 17, 23, 28, 34]; **Figs. 1a and 2**) The shoulder simulator consisted of up to six linear screw-driven actuators (Bimba, Monee, IL, USA) connected to 444-N load cells (Futek, Irvine, CA, USA). A universal strain gauge signal conditioner (Futek Model CSG110) was linked to a panel mount display (Futek Model IMP 650), and a test and measurement software (Sensit V2.5.1.0, Futek, Irvine, CA, USA) was used for load cell data acquisition in real time [1, 12, 28].

The specimen was mounted to the simulator on a jig with 6 degrees of freedom the scapula in 10° of anteflexion and 10° superior tilt of the glenoid, resulting in a 110° angle between the scapular spine and vertical axis [34]. The anatomical lines of action of the three portions of the deltoid, the SSC, and the ISP/TM unit were routed using custom 7-mm-diameter frictionless pulleys. The cable attached to the SSP tendon was aligned with a tilt of 10° to the horizontal [34]. In order to mimic the native force vectors of each of the deltoid portions, the pulley for the anterior deltoid was placed over the tip of the coracoid process, 5 mm anteriorly to the anterolateral corner of the acromion. The middle deltoid pulley routed over a point 5 mm posteriorly to the anterolateral corner of the acromion. The posterior deltoid pulley was placed at the posterolateral edge of the acromion in line with the scapular spine [1, 12, 28, 34].

Motion analysis and dynamic biomechanical testing

In order to cover a 180° field of view, four infrared cameras (Vero v1.3, Vicon Motion Capture Systems, Centennial, CO, USA) were mounted around the dynamic shoulder simulator. Three optical markers, representing a stationary triad, were placed on the acromion. Care was taken to place its center meticulously in line with the pulley of the middle deltoid. Additionally, a second moving triad was mounted to the humeral shaft with its

Abstract · Zusammenfassung

Obere Extremität 2021 · 16:120–129 https://doi.org/10.1007/s11678-021-00622-3

D. P. Berthold · L. N. Muench · R. Bell · C. Uyeki · K. Zenon · A. D. Mazzocca · E. Obopilwe · M. P. Cote · A. B. Imhoff · K. Beitzel

Biomechanical consequences of isolated, massive and irreparable posterosuperior rotator cuff tears on the glenohumeral joint. A dynamic biomechanical investigation of rotator cuff tears

Abstract

Background. Complex interactions between dynamic and static stabilizers of the shoulder girdle are critical for a biomechanically complex system, allowing for sufficient range of motion in multiple planes. This study assessed the biomechanical consequences of non-retracted rotator cuff tears (RCT), isolated and massive RCT, and irreparable, retracted posterosuperior RCT on the glenohumeral joint using a validated, dynamic shoulder testing system.

Methods. Eight fresh-frozen cadaveric shoulders were tested using a dynamic shoulder simulator. Each shoulder was tested in the following conditions: (1) intact state; (2) isolated non-retracted supraspinatus tendon (SSP) defect; (3) isolated non-retracted subscapularis tendon (SSC) defect; (4) isolated non-retracted infraspinatus tendon (ISP) defect; (5) massive non-retracted RCT involving all three tendons; (6) irreparable, retracted posterosuperior RCT.

Results. The SSP, SSC, and ISP simulated defects showed a significant increase in total deltoid force, respectively ($p = 0.012$; $p = 0.007$; $p = 0.001$). Compared with the intact state, the massive RCT showed a significant decrease in glenohumeral abduction angle ($p < 0.001$) and a significant increase in total deltoid force ($p < 0.001$). The irreparable, retracted posterosuperior RCT showed a significant decrease in glenohumeral abduction angle, significant increase of total deltoid force, subacromial peak contact pressure, and glenohumeral superior translation ($p > 0.001$, respectively) compared with the intact state.

Conclusion. In a dynamic biomechanical shoulder model, isolated non-retracted RCT, located lateral to the rotator cable, can be sufficiently compensated by the remaining intact cuff. However, in irreparable, massively retracted posterosuperior RCT located medial to the rotator cable, devasting effects on the glenohumeral joint can be expected and surgery should be recommended for these patients.

Keywords

Rotator cuff injuries · Biomechanics · Dynamic shoulder simulator · Superior capsule · Rotator cable

Biomechanische Auswirkungen von isolierten, massiven sowie irreparablen posterosuperioren Rotatorenmanschettenrupturen auf das glenohumerale Gelenk. Eine dynamische biomechanische Studie über Rotatorenmanschettenrupturen

Zusammenfassung

Hintergrund. Ein komplexes Zusammenspiel zwischen dynamischen und statischen Stabilisatoren des Schultergürtels ist von großer Bedeutung für ein biomechanisch komplexes System, um einen optimalen Bewegungsumfang des Schultergürtels in mehreren Ebenen zu ermöglichen. Ziel der Studie war es, mithilfe eines validierten dynamischen Schultermodells die biomechanischen Folgen nichtretrahierter (Patte I), isolierter und massiver Rotatorenmanschettenrisse („rotator cuff tear"; RCT) sowie retrahierter (Patte III), irreparabler, posterosuperiorer RCT auf das Glenohumeralgelenk zu untersuchen.

Material und Methoden. Dazu wurden 8 frisch gefrorene Spenderschultern in einem dynamischen Schultermodell getestet. Jede Spenderschulter durchlief die folgenden Testkonditionen (1) intakter Zustand; (2) isolierter, nichtretrahierter Supraspinatussehnen(SSP)-Defekt; (3) isolierter, nichtretrahierter Subskapularissehnen(SSC)-Defekt; (4) isolierter, nichtretrahierter Infraspinatussehnen(ISP)-Defekt; (5) nichtretrahierter, massiver RCT mit Beteiligung aller 3 Sehnen; (6) irreparabler, retrahierter, posterosuperiorer RCT.

Ergebnisse. Die simulierten SSP-, SSC- und ISP-Defekte zeigten einen signifikanten Anstieg der kumulativen Deltakraft ($p = 0{,}012$; $p = 0{,}007$; $p = 0{,}001$). Im Vergleich zum intakten Zustand zeigte der massive RCT eine signifikante Abnahme des glenohumeralen Abduktionswinkels ($p < 0{,}001$) sowie eine signifikante Zunahme der kumulativen Deltakraft ($p < 0{,}001$). Im Vergleich zum intakten Zustand zeigte der irreparable, retrahierte posterosuperiore RCT eine signifikante Abnahme des glenohumeralen Abduktionswinkels sowie einen signifikanten Anstieg der kumulativen Deltakraft, des subakromialen Spitzenkontaktdrucks und der glenohumeralen superioren Translation ($p > 0{,}001$).

Schlussfolgerung. Im dynamischen biomechanischen Schultermodell kann ein isolierter, nichtretrahierter RCT, welcher sich lateral des Rotatorenkabels befindet, durch die restliche intakte Manschette ausreichend kompensiert werden. Bei irreparablen, massiv retrahierten posterosuperioren RCT, welche sich medial des Rotatorenkabels befinden, sind jedoch verheerende Auswirkungen auf das Glenohumeralgelenk zu erwarten. Bei solchen Patienten sollte eine operative Versorgung empfohlen werden.

Schlüsselwörter

Rotatorenmanschettenläsionen · Biomechanik · Dynamisches Schultermodell · Superiore Kapsel · Rotatorenkabel

longitudinal axis, being in line with the center of the stationary triad placed on the acromion. In a displacement-controlled setting, a validated computer software (SiNet Hub Programmer V1.29; Applied Motion Products, Inc., CA, USA) was utilized to generate custom motion profiles for the individual actuator of the anterior, middle, and posterior deltoid as well of the SSP for each specimen, separately [1, 12, 28]. Next, a three-dimensional (3D) motion-tracking system (Vicon Nexus 2.8, Vicon Motion Capture Systems, Oxford, UK) and the four infrared cameras (Vicon Vero v1.3; frame rate of 250 Hz; position accuracy of 0.01 mm and 0.1°), recorded each motion profile of abduction of the arm from 0 to 60° in the scapular plane in neutral rotation. The scapula remained fixed to the shoulder simulator, corresponding to approximately 90° of total shoulder abduction [1, 12, 28]. For the calculation of each individual custom motion pro-

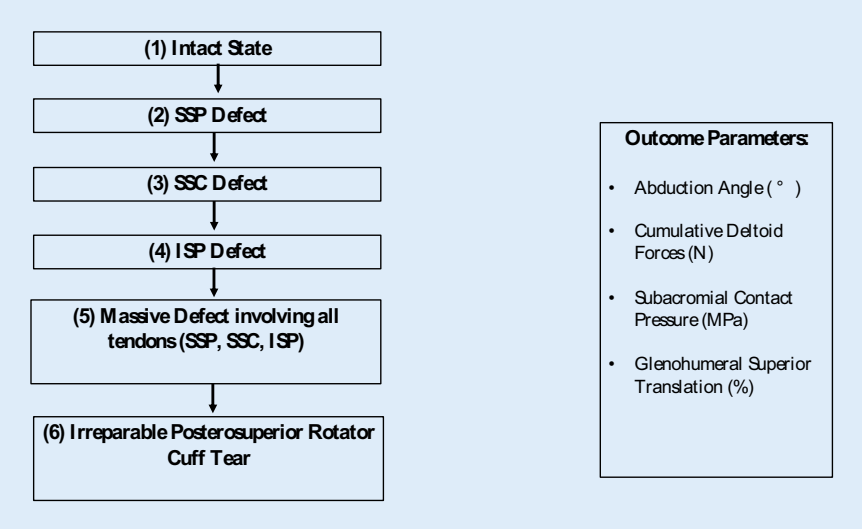

Fig. 2 ▲ Flowchart displaying the six testing conditions and the four outcome measures. *ISP* infraspinatus, *SSC* subscapularis, *SSP* supraspinatus

Fig. 3 ▲ Figure demonstrating the irreparable, massively retracted posterosuperior rotator cuff tear (Patte III)

file, the SSC and ISP/TM unit was loaded statically with a 1.36-kg hanging weight, allowing for a balanced abduction motion [26]. To generate reliable data of applied forces, each motion cycle was repeated three times [1, 12, 28], by applying 10 N to the SSP as well as the anterior, middle, and posterior deltoid, respectively, to center the joint at the resting position [1, 12, 28, 33].

Each testing cycle started with the specimen in its resting position in 0° of abduction and neutral rotation. As such, individual tendon excursion and velocity were calculated to reach 60° of glenohumeral abduction, as previously described [10, 28]. All tendons reached the abduction angle simultaneously while force in each muscle was specified to increase linearly [28]. To ensure reliability, a unique motion profile was generated in the intact state (condition 1) and maintained throughout all further testing conditions for each individual shoulder.

Testing conditions

The specimens remained in the dynamic shoulder simulator throughout all testing conditions. To avoid performance bias, all procedures were performed by the same surgeon. In total, every specimen underwent six different conditions with each specimen being its own control (**Fig. 2**):

1. Intact state
2. Non-retracted (according to Patte I) SSP defect
3. Non-retracted SSC defect
4. Non-retracted ISP defect
5. Non-retracted massive RCT involving all three tendons
6. Irreparable, massive retracted (according to Patte III) posterosuperior RCT

First, the specimen was tested in the (1) native, intact state. Secondly, a (2) non-retracted (Patte I) SSP defect was created by releasing the pulley from the muscle belly. Third, a (3) non-retracted (Patte I) SSC defect was created by releasing the pulley from the muscle belly. Fourth, the SSC was re-attached to the pulley, and a (4) non-retracted (Patte I) ISP defect was simulated, also by releasing the pulley from the muscle belly. Fifth (5), each muscle belly (SSP, ISP, SSC) was released from its pulley and a massive, non-retracted (Patte I) RCT was simulated. Lastly, each pulley was re-attached and an (6) irreparable, massively retracted (Patte III) posterosuperior RCT was created by sharply dissecting the footprint of the supraspinatus and cranial part of the infraspinatus on the greater humeral tuberosity (**Fig. 3**). Subsequently, the supraspinatus muscle belly was detached from the supraspinatus fossa in order to create a massively retracted RCT (Patte III).

Outcome parameters

Four parameters were directly measured in each cadaveric shoulder for each testing condition:

1. Maximum glenohumeral abduction angle (°)
2. Glenohumeral superior translation (%)
3. Subacromial peak contact pressure (MPa)
4. Cumulative deltoid force (N) [1, 12, 28]

As previously described, glenohumeral abduction angle and glenohumeral superior translation were measured using 3D motion tracking (Vicon Nexus 2.8, Vicon Motion Capture Systems, Oxford, UK) and four infrared cameras (Vicon Vero v1.3). Glenohumeral superior translation for conditions 2–6 was calculated by dividing each value by the value for the native, intact condition (1) [28]. By using a pressure-measuring system (saturation pressure, 0.56 MPa; pressure-mapping sensor model 4205 Tekscan), subacromial peak contact pressure was mea-

Table 1 Maximum glenohumeral abduction (ABD angle), mean cumulative deltoid force (*Force*), mean subacromial peak contact pressure (*Pressure*), and mean glenohumeral superior translation (*ghST*) for each testing condition

Intact		SSP defect		SSC defect		ISP defect		Massive defect		Posterosuperior defect	
ABD angle (°)	ABD angle (%)	ABD angle (°)	ABD angle (%)	ABD angle (°)	ABD angle (°)	ABD angle (%)	ABD angle (%)	ABD angle (°)	ABD angle (%)	ABD angle (°)	ABD angle (%)
56 ± 3	100	55 ± 2	98	54 ± 3	96	54 ± 2[a]	96	51 ± 2[a]	91	34 ± 3[a]	61
Force (N)	Force (%)	Force (N)	Force (%)	Force (N)	Force (N)	Force (%)	Force (%)	Force (N)	Force (%)	Force (N)	Force (%)
183 ± 15	100	199 ± 28[a]	109	200 ± 35[a]	109	207 ± 21[a]	113	204 ± 17[a]	111	221 ± 20[a]	121
Pressure (MPa)	Pressure (MPa)	Pressure (%)	Pressure (MPa)	Pressure (%)	Pressure (MPa)	Pressure (%)	Pressure (MPa)	Pressure (%)	Pressure (MPa)	Pressure (%)	Pressure (MPa)
0.25 ± 0.08	100	0.32 ± 0.10	128	0.38 ± 0.14	152	0.37 ± 0.13	148	0.36 ± 0.12	144	0.74 ± 0.47[a]	296
–	ghST (%)	–	ghST (%)	–	ghST (%)	–	ghST (%)	–	ghST (%)	–	ghST (%)
–	100	–	103	–	105	–	103	–	105	–	159[a]

Values are given as mean ± standard error; % glenohumeral abduction, % cumulative deltoid force, and % subacromial contact pressure were calculated by dividing each value by the value for the native, intact condition; % glenohumeral superior translation was calculated by dividing each value by the value for condition 1

ABD abduction angle, *ghST* glenohumeral superior translation, *ISP* infraspinatus, *SSC* subscapularis, *SSP* supraspinatus

[a]Significant difference compared with condition 1

sured between the coracoacromial arch (coracoacromial ligament and acromion) and the humerus throughout abduction [1, 22, 28]. Deltoid force was recorded in real time throughout ROM by load cells (Futek) connected to the actuators [1, 12, 28], while cumulative deltoid force was calculated as the summation of anterior, middle, and posterior deltoid forces. Every specimen underwent three trials for each measurement [1, 12, 28].

Statistical analysis

Based on previous, validated biomechanical studies, a priory power analysis was performed to determine detectable differences in the dependent variables given estimated standard deviations [28]. For the glenohumeral abduction angle, an error variance of 1° across all conditions with a correlation of 0.3 between measurements was assumed. A sample size of six specimens will provide 80% power to detect a 1° difference in shoulder angle at an α level of 0.05.

Descriptive statistics including mean and standard deviation were calculated to characterize the specimens. Repeated measures analysis of variance was performed to examine differences in maximal glenohumeral abduction angle, glenohumeral superior translation, subacromial peak contact pressure, and cumulative deltoid force among the various testing conditions. There were six comparisons of interest. For simplicity, the adjusted p values are reported. Specifically, the unadjusted p values were multiplied by 6. When significant, post hoc paired t tests with a Bonferroni corrected alpha were performed to determine which pairwise comparisons were statistically significant. The p value for the omnibus analysis of variance was $p < 0.001$ for each outcome measure. Given that there was only one independent variable (intact state; SSP defect; SSC defect; ISP defect; massive RCT; irreparable posterosuperior RCT), an interaction term was not included since a second independent variable would have been required. The alpha level for all analyses was set at 0.05. All statistical analyses were performed using Stata 15.2 software (StataCorp 2017; Stata Statistical Software: Release 15, StataCorp LLC, College Station, TX, USA).

Results

Intact shoulders

Intact shoulders achieved a mean maximum glenohumeral abduction of 56 ± 3°, requiring on average 183 ± 15 N of total deltoid force, while subacromial peak contact pressure was 0.25 ± 0.08 MPa (**Table 1**; **Figs. 4**, **5**, **6** and **7**).

Simulated rotator cuff tears

The SSP, SSC, and ISP simulated defects showed a significant increase in total deltoid force ($p = 0.012$, $p = 0.007$, $p = 0.001$, respectively). Additionally, only the ISP defect state showed a significant decrease in glenohumeral abduction angle ($p = 0.045$). Glenohumeral superior translation was comparable ($p =$ n. s.) between the intact state and the simulated RCT (**Table 1**; **Figs. 4**, **5**, **6** and **7**).

Massive rotator cuff tears

Compared with the intact state, the massive, non-retracted RCT showed a significant decrease in glenohumeral abduction angle ($p < 0.001$) and a significant increase in total deltoid force ($p < 0.001$). Glenohumeral superior translation and subacromial peak contact pressure was comparable between the simulated massive RCT and the intact state ($p =$ n. s.; **Table 1**; **Figs. 4**, **5**, **6** and **7**).

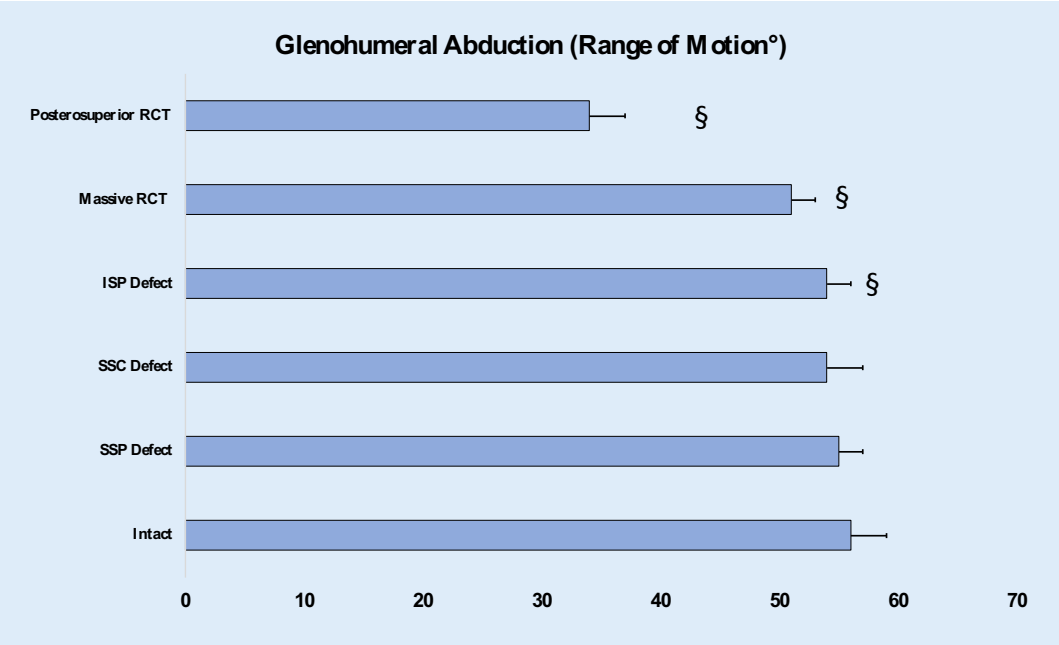

Fig. 4 ◄ Glenohumeral abduction (range of motion °) across the testing conditions. §Significant difference compared with condition 1 (intact). *RCT* rotator cuff tear, *ISP* infraspinatus, *SSC* subscapularis, *SSP* supraspinatus

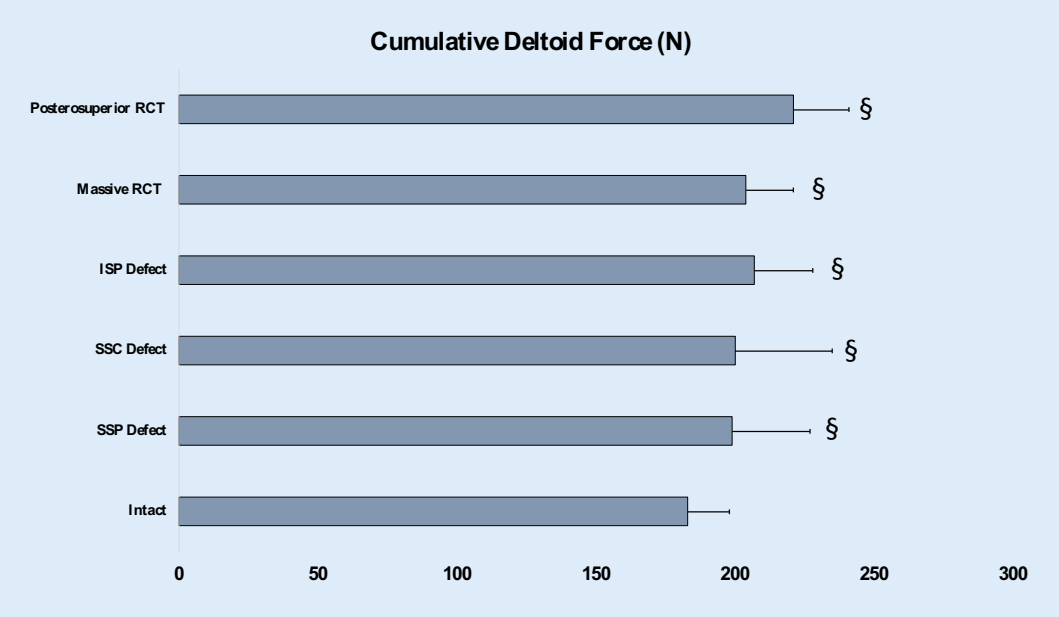

Fig. 5 ◄ Maximum cumulative deltoid force (*N*) across the testing conditions. §Significant difference compared with condition 1. *RCT* rotator cuff tear, *ISP* infraspinatus, *SSC* subscapularis, *SSP* supraspinatus

Irreparable posterosuperior rotator cuff tears

The irreparable, massively retracted posterosuperior RCT showed a significant decrease in glenohumeral abduction angle, as well as a significant increase in total deltoid force, subacromial peak contact pressure, and glenohumeral superior translation (all $p > 0.001$) compared with the intact state (**Table 1**; **Figs. 4**, **5**, **6** **and 7**).

Discussion

The most important finding of this study was that an isolated, non-retracted RCT lateral to the rotator cable can be sufficiently compensated by the remaining, intact cuff in a dynamic biomechanical shoulder model. Additionally, when facing irreparable, massively retracted posterosuperior RCT medial to the rotator cable, devasting effects on the glenohumeral joint can be expected. These include increased maximum deltoid forces, which can lead to increased deltoid fatigue over time, and consistently increased subacromial peak contact pressure. This could enhance abrasive glenoid wear, resulting in decreased shoulder function, pain, and weakness. In these patients, restoring the integrity of the muscular force couple and preventing superior humeral head migration are highly recommended to reduce the risk of the aforementioned symptoms, secondary to RCT.

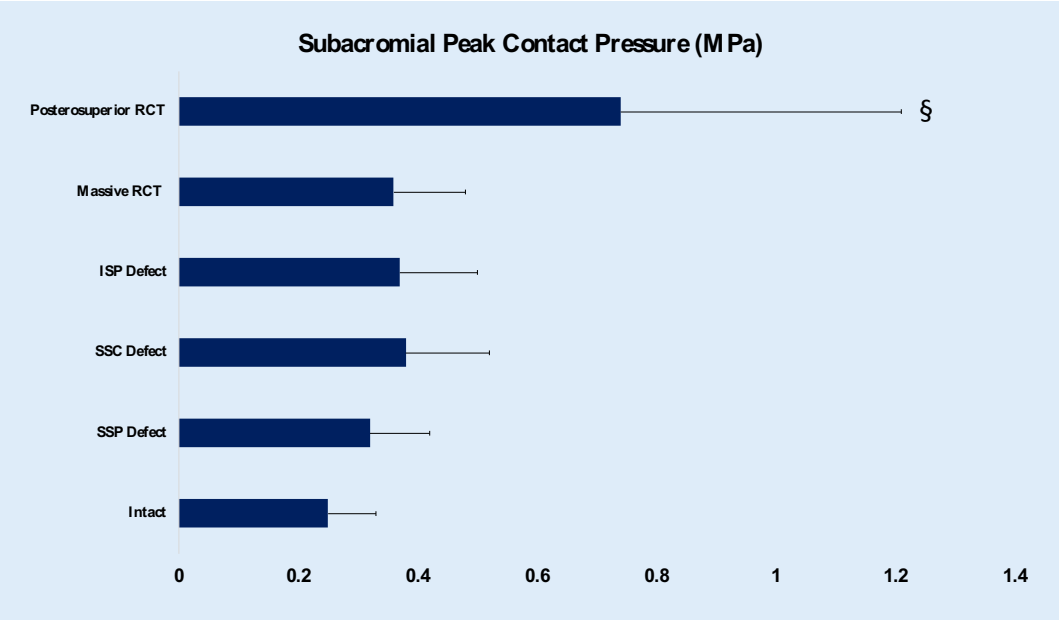

Fig. 6 ◄ Subacromial peak contact pressure (MPa) across the testing conditions. §Significant difference compared with condition 1. *RCT* rotator cuff tear, *ISP* infraspinatus, *SSC* subscapularis, *SSP* supraspinatus

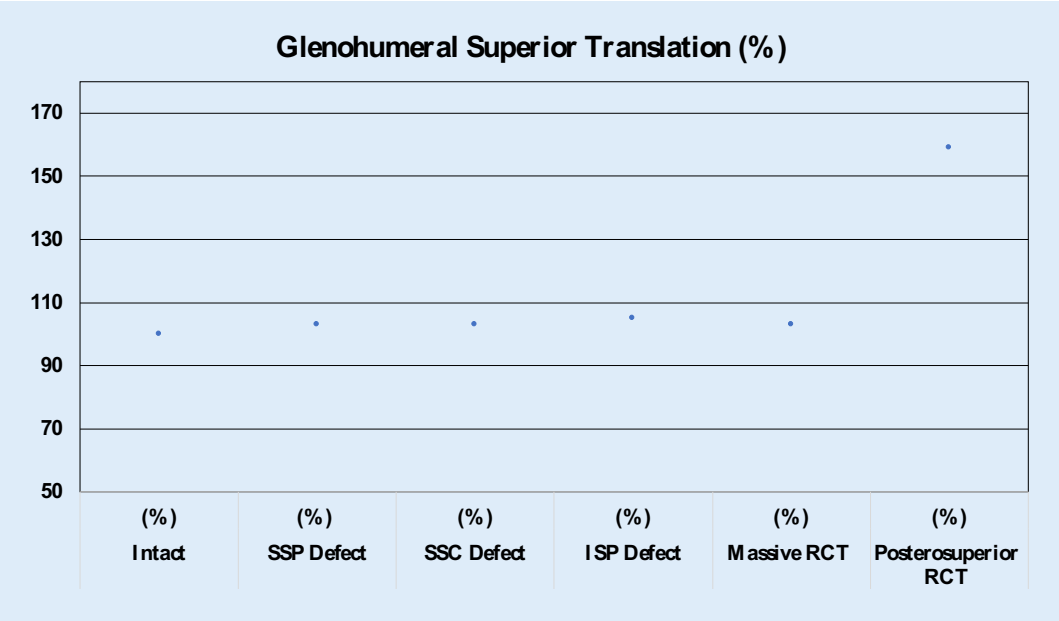

Fig. 7 ◄ Changes (in %) across the testing conditions for glenohumeral superior translation. *RCT* rotator cuff tear, *ISP* infraspinatus, *SSC* subscapularis, *SSP* supraspinatus

A solid understanding of both native and defect shoulder kinematics is key to approaching rotator cuff surgery. This includes the complex interactions between static and dynamic stabilizers of the glenohumeral joint that are needed to provide full ROM and sufficient shoulder function. The glenohumeral joint has the greatest ROM of any joint in the human body; however, this is accompanied by an increased risk of joint instability [21] Therefore, synergistic and coordinated action between these stabilizers is critical for producing a biomechanically complex system to ensure sufficient ROM in multiple planes.

During glenohumeral abduction, the rotator cuff applies a compressive load to the glenohumeral joint [20, 21]. The small glenoid fossa and the increased laxity of the glenohumeral joint play an important role in providing ROM; however, they are also more susceptible to joint instability [21]. As such, Lippit et al. were among the first to advocate the concept of joint concavity compression in providing glenohumeral joint stability, especially in the functional positions where the glenohumeral ligaments are lax [20, 21]. Thus, an intact rotator cuff is needed to ensure optimal concavity compression. In cases of retracted tears involving the rotator cuff medial to the rotator cable, glenohumeral joint instability may result, often leading to superior humeral head migration. In these patients, activation of the deltoid muscle results in a shearing force on the humeral head and corresponding proximal migration at lower abduction angles, due to the absence of the rotator cuff [29]. Likewise, at higher abduction angles, the resultant force vector from the

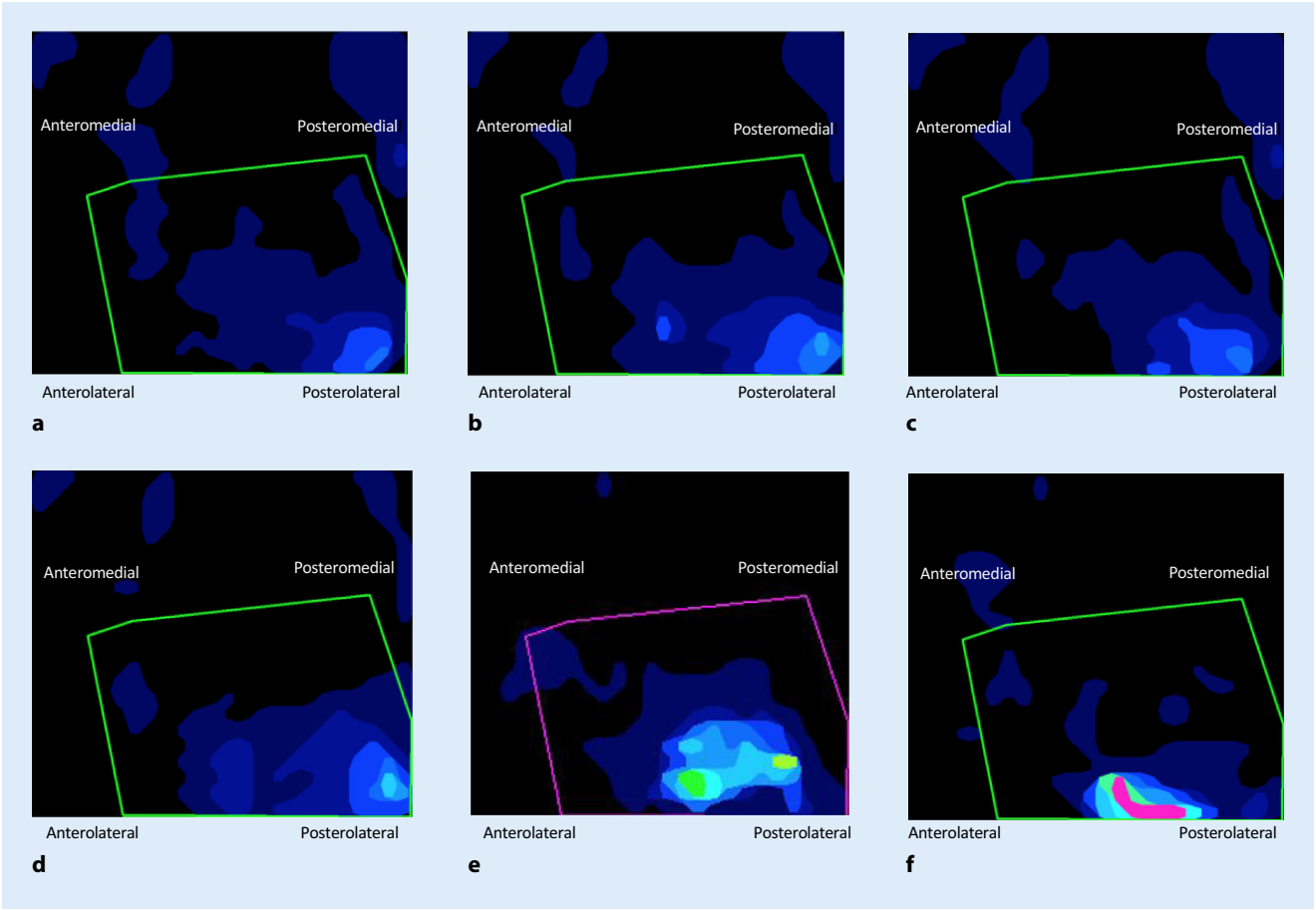

Fig. 8 ▲ Changes in subacromial peak contact pressure along the six testing conditions. The subacromial space is displayed by the *green* and *purple box*. **a** Intact state; most of the peak pressure is located at the posterolateral acromion; **b** a slight increase in peak contact pressure is demonstrated for the supraspinatus defect state; in subscapularis (**c**) or infraspinatus (**d**) tears, the force couple is disrupted, which results in decentering of the humeral head; **e** a massive tear involving all of the tendons results in a noticeable increase in subacromial contact pressure; **f** the consequences of an irreparable, posterosuperior rotator cuff tear with decentering of the humeral head and increase in subacromial contact pressure

deltoid muscle is not directed superiorly, but instead is directed medially or horizontally into the glenoid, contributing to the concavity compression force [29].

An important consideration from this biomechanical study is that the supraspinatus is the dominant muscle during the first 30° of abduction. As such, the anterior and middle deltoid are considered to have their preferential muscle activity and loading from 30 to 90° of glenohumeral abduction [2, 25]. In patients with RCT, kinematic alterations and subsequent impairing of the biomechanical synergy between deltoid and rotator cuff muscles may occur [18]. Therefore, a greater amount of force on the middle deltoid can be expected in these patients, most notably between 10 and 45° of abduction [12, 14, 24]. While greater deltoid forces are required to maintain joint stability with a significant decrease in glenohumeral abduction, an insufficient mechanical advantage of the deltoid may occur [12, 24, 30]. This was noted in a recent biomechanical investigation by Dyrna et al. [12], who highlighted the required compensatory deltoid function to make up for abduction motion loss in the presence of simulated RCT.

Another important biomechanical consideration is the concept of a balanced force couple. The ISP/TM, SSC, and SSP act as a muscular force couple providing glenohumeral joint stability and contributing to humeral head centration in the axial plane [6–8, 13]. Similarly, the three portions of the deltoid and the inferior portion of the rotator cuff provide the force couple in the coronal plane. In cases of isolated SSC or ISP/TM tears, the force couple may not be established, which results in decentering of the humeral head (**Fig. 8**). However, in cases of isolated SSP tears and an intact rotator cable, an intact force couple may allow for centered shoulder kinematics during abduction, as the rotator cable maintains the "suspension bridge" [7]. In large defects of the supraspinatus, an intact force couple stabilizes the humeral head by acting as a fulcrum during abduction. However, the force couple can be affected as rotator cuff tears progress to the anterior or posterior portions of the rotator cuff [12], which further impairs shoulder function during abduction motion [5].

As mentioned previously, unstable fulcrum kinematics, seen in massive tears of the superior and posterior cuff, often present with uncoupling of the essential force couples. This can lead to an unstable fulcrum of motion [5] and highly restricted active shoulder motion [5]. Lastly, patients with massive tears that involve all of the supraspinatus, more than one third of the posterior cuff, and at least one half of the subscapularis, have difficulty centering the humeral head on the glenoid, resulting in a superior subluxation of the humeral head.

The main differences between the irreparable and reparable condition is that for the reparable condition, the native cuff is still in place, which acts firstly as a subacromial spacer or "pillow" by filling the subacromial space. In the massive non-retracted condition, since both the transverse and coronal force couple is not given and the rotator cable may be insufficient, the vector of the deltoid may not change as the spacer effect is still in place. As such, no increase in superior humeral migration or subacromial peak contact pressure is expected in this dynamic biomechanical investigation. However, when removing the cuff, the subacromial spacer effect is lost, and the vector of the deltoid is now directed horizontally into the glenoid, which increases superior head migration and subsequent subacromial contact pressure [11]. This observation shows the importance of the native rotator cuff having a natural spacer effect and ensuring humeral head containment.

Additionally, abnormal joint loading secondary to RCT can lead to bony alterations such as erosion of the glenoid and the humeral head, or in the case of severe rotator cuff arthropathy, to an acetabularization of the acromion [27]. This can lead to anterosuperior escape and mechanical conflict between the humeral head, the superior glenoid, and the acromion [9]. As a result, severe osteoarthritis and collapse of cartilage and bony structures may result in pain and limited shoulder function [27]. Abnormal joint loading also contributes to changes in peak glenoidal pressure, leading to erosion of the glenoid. In some cases, the pressure might be oriented within the postero-inferior region, rather than the supero-inferior axis of the glenoid, leading to a type B glenoid, according to Walch et al. [4, 19].

Lastly, the location of the RCT may be more important than tear size in shoulder kinematics. In general, most RCT involve the supraspinatus and some portion of the posterior rotator cuff. In these cases, a normal transverse plane force couple allows for normal function. However, if the posterior rotator cuff is damaged, a stable fulcrum may not be established, which could lead to the aforementioned effects.

Limitations

This study has several limitations. As this is a biomechanical cadaveric study, all data represent a time-zero condition without randomization of the testing order. Additionally, in this biomechanical model, only the rotator cuff and deltoid muscles were simulated. However, the pectoralis major and latissimus dorsi tendon, which also play a role in superior glenohumeral stability, were unloaded. Additionally, one loading rate was investigated, while equal loads through each deltoid head were assumed. Of importance, the mean glenohumeral abduction of intact shoulders was only 56° (not 60°), which indicated that even in the intact situation 60° were not reached. Finally, as it is necessary to securely mount the specimen to the shoulder simulator, any scapulothoracic motion was eliminated due to said fixation.

Practical conclusion

- **In a dynamic biomechanical shoulder model, isolated non-retracted rotator cuff tear (RCT) located lateral to the rotator cable can be sufficiently compensated by the remaining, intact cuff.**
- **However, in irreparable, massively retracted posterosuperior RCT located medial to the rotator cable, devasting effects on the glenohumeral joint can be expected including increased maximum deltoid forces, increased subacromial peak contact pressure, and decreased shoulder function.**
- **In patients with retracted tears involving the cuff located medial to the rotator cable, surgery should be highly recommended to improve shoulder function.**

Corresponding address

Daniel P. Berthold, MD
Department of Orthopedic Sports Medicine, Technical University of Munich
Ismaninger Str. 22, 81675 Munich, Germany
daniel.berthold@tum.de

Funding. The University of Connecticut Health Center/UConn Musculoskeletal Institute has received direct funding and material support from Arthrex Inc. (Naples, FL, USA). The company and the society had no influence on study design, data collection, or interpretation of the results or the final manuscript.

Compliance with ethical guidelines

Conflict of interest. A.D. Mazzocca is a consultant for Orthofix and Arthrex and receives research grants from Arthrex. M.P. Cote receives personal fees from the Arthroscopy Association of North America (AANA). K. Beitzel is a consultant for Arthrex. D.P. Berthold, L.N. Muench, R. Bell, C. Uyeki, K. Zenon, E. Obopilwe, and A.B. Imhoff declare that they have no competing interests.

Ethical approval was obtained via Human Research Determination Form to the institutional review board (IRB) of the University of Connecticut and it was documented that no IRB approval was required (de-identified specimen do not constitute human subjects research).

References

1. Adams CR, Comer B, Scheiderer B, Imhoff FB, Morikawa D, Kia C, Muench LN, Baldino JB, Mazzocca AD (2020) The effect of glenohumeral fixation angle on deltoid function during superior capsule reconstruction: a biomechanical investigation. Arthroscopy 36:400–408
2. Alpert SW, Pink M, Jobe FW, McMahon PJ, Mathiyakom W (2000) Electromyographic analysis of deltoid and rotator cuff function under varying loads and speeds. J Shoulder Elbow Surg 9:47–58
3. Bedi A, Dines J, Warren RF, Dines DM (2010) Massive tears of the rotator cuff. J Bone Joint Surg Am 92:1894–1908
4. Beuckelaers E, Jacxsens M, Van Tongel A, De Wilde LF (2014) Three-dimensional computed tomography scan evaluation of the pattern of erosion in type B glenoids. J Shoulder Elbow Surg 23:109–116
5. Burkhart SS (1992) Fluoroscopic comparison of kinematic patterns in massive rotator cuff tears. A suspension bridge model. Clin Orthop Relat Res 284:144–152
6. Burkhart SS (1994) Reconciling the paradox of rotator cuff repair versus debridement: a unified

biomechanical rationale for the treatment of rotator cuff tears. Arthroscopy 10:4–19
7. Burkhart SS, Esch JC, Jolson RS (1993) The rotator crescent and rotator cable: an anatomic description of the shoulder's "suspension bridge". Arthroscopy 9:611–616
8. Burkhart SS, Nottage WM, Ogilvie-Harris DJ, Kohn HS, Pachelli A (1994) Partial repair of irreparable rotator cuff tears. Arthroscopy 10:363–370
9. Collins DN, Harryman DT (1997) Arthroplasty for arthritis and rotator cuff deficiency. Orthop Clin North Am 28:225–239
10. Debski RE, McMahon PJ, Thompson WO, Woo SL, Warner JJ, Fu FH (1995) A new dynamic testing apparatus to study glenohumeral joint motion. J Biomech 28:869–874
11. Dyrna F, Berthold DP, Muench LN, Beitzel K, Kia C, Obopilwe E, Pauzenberger L, Adams CR, Cote MP, Scheiderer B, Mazzocca AD (2020) Graft tensioning in superior capsular reconstruction improves glenohumeral joint kinematics in massive irreparable rotator cuff tears: a biomechanical study of the influence of superior capsular reconstruction on dynamic shoulder abduction. Orthop J Sports Med 8:2325967120957424
12. Dyrna F, Kumar NS, Obopilwe E, Scheiderer B, Comer B, Nowak M, Romeo AA, Mazzocca AD, Beitzel K (2018) Relationship between deltoid and rotator cuff muscles during dynamic shoulder abduction: a biomechanical study of rotator cuff tear progression. Am J Sports Med 46:1919–1926
13. Greenspoon JA, Petri M, Warth RJ, Millett PJ (2015) Massive rotator cuff tears: pathomechanics, current treatment options, and clinical outcomes. J Shoulder Elbow Surg 24:1493–1505
14. Hansen ML, Otis JC, Johnson JS, Cordasco FA, Craig EV, Warren RF (2008) Biomechanics of massive rotator cuff tears: implications for treatment. J Bone Joint Surg Am 90:316–325
15. Harryman DT, Mack LA, Wang KY, Jackins SE, Richardson ML, Matsen FA (1991) Repairs of the rotator cuff. Correlation of functional results with integrity of the cuff. J Bone Joint Surg Am 73:982–989
16. Henninger HB, Barg A, Anderson AE, Bachus KN, Tashjian RZ, Burks RT (2012) Effect of deltoid tension and humeral version in reverse total shoulder arthroplasty: a biomechanical study. J Shoulder Elbow Surg 21:483–490
17. Hurschler C, Wülker N, Mendila M (2000) The effect of negative intraarticular pressure and rotator cuff force on glenohumeral translation during simulated active elevation. Clin Biomech (Bristol, Avon) 15:306–314
18. Kijima T, Matsuki K, Ochiai N, Yamaguchi T, Sasaki Y, Hashimoto E, Sasaki Y, Yamazaki H, Kenmoku T, Yamaguchi S, Masuda Y, Umekita H, Banks SA, Takahashi K (2015) In vivo 3-dimensional analysis of scapular and glenohumeral kinematics: comparison of symptomatic or asymptomatic shoulders with rotator cuff tears and healthy shoulders. J Shoulder Elbow Surg 24:1817–1826
19. Knowles NK, Keener JD, Ferreira LM, Athwal GS (2015) Quantification of the position, orientation, and surface area of bone loss in type B2 glenoids. J Shoulder Elbow Surg 24:503–510
20. Lippitt S, Matsen F (1993) Mechanisms of glenohumeral joint stability. Clin Orthop Relat Res 291:20–28
21. Lippitt SB, Vanderhooft JE, Harris SL, Sidles JA, Harryman DT II, Matsen FA III (1993) Glenohumeral stability from concavity-compression: a quantitative analysis. J Shoulder Elbow Surg 2:27–35
22. Mihata T, McGarry MH, Kahn T, Goldberg I, Neo M, Lee TQ (2016) Biomechanical effect of thickness and tension of fascia Lata graft on glenohumeral stability for superior capsule reconstruction in irreparable supraspinatus tears. Arthroscopy 32(2):418–426
23. Mihata T, McGarry MH, Pirolo JM, Kinoshita M, Lee TQ (2012) Superior capsule reconstruction to restore superior stability in irreparable rotator cuff tears: a biomechanical cadaveric study. Am J Sports Med 40:2248–2255
24. Oh JH, Jun BJ, McGarry MH, Lee TQ (2011) Does a critical rotator cuff tear stage exist?: a biomechanical study of rotator cuff tear progression in human cadaver shoulders. J Bone Joint Surg Am 93:2100–2109
25. Otis JC, Jiang CC, Wickiewicz TL, Peterson MG, Warren RF, Santner TJ (1994) Changes in the moment arms of the rotator cuff and deltoid muscles with abduction and rotation. J Bone Joint Surg Am 76:667–676
26. Poitras P, Kingwell SP, Ramadan O, Russell DL, Uhthoff HK, Lapner P (2010) The effect of posterior capsular tightening on peak subacromial contact pressure during simulated active abduction in the scapular plane. J Shoulder Elbow Surg 19:406–413
27. Rugg CM, Gallo RA, Craig EV, Feeley BT (2018) The pathogenesis and management of cuff tear arthropathy. J Shoulder Elbow Surg 27:2271–2283
28. Scheiderer B, Kia C, Obopilwe E, Johnson JD, Cote MP, Imhoff FB, Dyrna F, Beitzel K, Imhoff AB, Adams CR (2020) Biomechanical effect of superior capsule reconstruction using a 3-mm and 6-mm thick acellular dermal allograft in a dynamic shoulder model. Arthroscopy 36:355–364
29. Singh S, Reeves J, Langohr GDG, Johnson JA, Athwal GS (2019) The subacromial balloon spacer versus superior capsular reconstruction in the treatment of irreparable rotator cuff tears: a biomechanical assessment. Arthroscopy 35:382–389
30. Terrier A, Reist A, Vogel A, Farron A (2007) Effect of supraspinatus deficiency on humerus translation and glenohumeral contact force during abduction. Clin Biomech (Bristol, Avon) 22:645–651
31. Thompson WO, Debski RE, Boardman ND 3rd, Taskiran E, Warner JJ, Fu FH, Woo SL (1996) A biomechanical analysis of rotator cuff deficiency in a cadaveric model. Am J Sports Med 24:286–292
32. Tokish JM, Alexander TC, Kissenberth MJ, Hawkins RJ (2017) Pseudoparalysis: a systematic review of term definitions, treatment approaches, and outcomes of management techniques. J Shoulder Elbow Surg 26:e177–e187
33. Veeger HE, Van der Helm FC, Van der Woude LH, Pronk GM, Rozendal RH (1991) Inertia and muscle contraction parameters for musculoskeletal modelling of the shoulder mechanism. J Biomech 24:615–629
34. Wuelker N, Wirth CJ, Plitz W, Roetman B (1995) A dynamic shoulder model: reliability testing and muscle force study. J Biomech 28:489–499